NEUROSCIENCE

REVIEW

D. Campagner et al. / Neuroscience 368 (2018) 95–108

What the Whiskers Tell the Brain

Dario Campagner, Mathew H. Evans, Michaela S. E. Loft and Rasmus S. Petersen *

Division of Neuroscience & Experimental Psychology, Faculty of Biology, Medicine & Health, University of Manchester, Manchester M13 9PT, UK

Abstract—A fundamental question in the investigation of any sensory system is what physical signals drive its sensory neurons during natural behavior. Surprisingly, in the whisker system, it is only recently that answers to this question have emerged. Here, we review the key developments, focussing mainly on the first stage of the ascending pathway – the primary whisker afferents (PWAs). We first consider a biomechanical framework, which describes the fundamental mechanical forces acting on the whiskers during active sensation. We then discuss technical progress that has allowed such mechanical variables to be estimated in awake, behaving animals. We discuss past electrophysiological evidence concerning how PWAs function and reinterpret it within the biomechanical framework. Finally, we consider recent studies of PWAs in awake, behaving animals and compare the results to related studies of the cortex. We argue that understanding 'what the whiskers tell the brain' sheds valuable light on the computational functions of downstream neural circuits, in particular, the barrel cortex.

Key words: whisker system, somatosensory system, neural coding, trigeminal ganglion, barrel cortex, whisker mechanics.

INTRODUCTION

> *"It is extremely difficult to understand the visual cortex without understanding the retina and the lens. In the same way, it is difficult to understand the barrel cortex without understanding the follicle receptors and the whiskers".*
>
> [Fox, 2008]

The interface between world and brain consists of sensory receptors that transduce physical signals (chemical, electromagnetic, thermal or mechanical) into cellular signals. Our knowledge of sensory systems is rooted in the ability to investigate how such physical variables translate into the responses of sensory neurons, and in the understanding of what information the spike trains of primary sensory neurons provide to downstream neural circuits, including the cerebral cortex.

The mechanoreceptors that form the basis of the somatosensory system are transducers of mechanical forces applied to the body. Forces due to body–object contact deform tissues within which mechanoreceptive nerve endings are embedded – in the case of the whisker system, the whisker follicle (Ebara et al., 2002; Mitchinson et al., 2004; Lottem and Azouz, 2011; Whiteley et al., 2015; Takatoh et al., 2017).

A long-recognized obstacle to the study of somatosensation is that the fundamental mechanical forces are very difficult to measure directly. Instead, many studies have investigated the encoding of directly measurable and controllable 'kinematic' quantities - measures of whisker position and its temporal derivatives. However, kinematic quantities do not necessarily relate to the underlying forces in any simple fashion. This is illustrated by classic work on primary afferents that innervate the primate hand (Phillips and Johnson, 1982). A ridged surface pressed into the fingertip deforms the skin and elicits robust firing in Slowly Adapting (SA) primary afferents. The pattern of skin deformation (the kinematics) caused by object contact is markedly different to the pattern of load force exerted by the object on the skin surface: SA activity correlates poorly with the kinematic indentation pattern, but well with the load force pattern.

It was first recognized by Johnson and colleagues that biomechanical modeling offers a potential way round the force measurement problem (Phillips and Johnson, 1982). It is possible, using continuum mechanics, to make a biomechanical model of skin – that is, a system of equations that describes how the skin deforms upon application of a load force to its surface. If the skin is assumed to be a simple medium (elastic, homogeneous, isotropic and incompressible), the system of equations can be inverted to yield estimates of the load force (Phillips and Johnson, 1982; Sripati et al., 2006). The load force can, in principle, then be used to estimate tissue deformation (strain) inside the skin at the site of mechanoreceptive nerve endings. However, a substantial difficulty in taking this modeling approach further is that modeling the skin

*Corresponding author.
E-mail address: r.petersen@manchester.ac.uk (R. S. Petersen).

https://doi.org/10.1016/j.neuroscience.2017.08.005
0306-4522/

in a more realistic way has required finite-element simulations on supercomputers (Dandekar et al., 2003).

One of the lesser known beauties of the whiskers as a model system is that the force-kinematics relationship is much simpler than that for the hand. The two simple, but crucial, differences are that whiskers protrude from the skin and that they are near-conical objects, typically 10 times longer than their base width (Williams and Kramer, 2010; Hires et al., 2016). First, this allows a whisker's motion and shape to be directly measured, accurately and non-invasively, in the awake, behaving animal, by high-speed imaging. Second, the mathematical problem of how a long, thin rod deforms under an applied load is much simpler than the analogous problem for an arbitrary 3D body. There are simple, but powerful, results (detailed below) that express the relationship between the force applied to a rod and how much it bends (Birdwell et al., 2007; Pammer et al., 2013). By making appropriate measurements of whisker shape from imaging data, estimates of the mechanical forces acting on the base of the whisker shaft can be derived. These procedures were first applied ''ex vivo" using plucked whiskers mounted on motors (Birdwell et al., 2007), later in vivo (O'Connor et al., 2010; Bagdasarian et al., 2013; Pammer et al., 2013; Huet et al., 2015; Wallach et al., 2016) and, in a significant recent advance, to awake, behaving animals where neuronal activity is simultaneously measured (O'Connor et al., 2010b, 2013; Petreanu et al., 2012; Chen et al., 2013; Hires et al., 2015; Peron et al., 2015; Bush et al., 2016; Campagner et al., 2016; Severson et al., 2017).

It is the primary purpose of this article to review these developments and how they have advanced our knowledge of neural coding in primary whisker afferents (PWAs). The wider significance of this work is that it clarifies the computational problems of touch that downstream neural circuitry, including barrel cortex, have evolved to solve, and provides an essential baseline for investigation of the perceptual algorithms implemented in neural circuitry (Marr, 1982; Maravall and Diamond, 2014). We start by reviewing a general framework for whisker mechanics.

MECHANICAL FRAMEWORK FOR WHISKER-BASED SENSATION

In the absence of contact (''whisking in air"), whisker mechanoreceptors are potentially susceptible to diverse forces, reflecting inertia of the whisker, contraction of facial muscles and viscoelasticity of the whisker pad tissue within which the follicle is anchored. When a time-independent force is applied to a whisker, force onset triggers high-frequency vibration of the whisker (Neimark et al., 2003; Hartmann et al., 2003; Ritt et al., 2008; Wolfe et al., 2008; Boubenec et al., 2012), which rapidly decays to a static equilibrium, where the whisker bends against the object (Birdwell et al., 2007). In steady state, the degree of bending depends on both the applied force and the whisker's stiffness. During active whisking against an object, the relative importance of the dynamic and static effects depends on the material properties of the whisker, the whisker motion, the shape/texture/material of the object and where along the whisker shaft the motion of the whisker is measured. Since mechanoreceptors sense stresses at the base of a whisker, it is motion here, rather than at the tip, that is most relevant to neural coding in PWAs. Whisking against a rough surface elicits dynamic 'slip-stick' effects that evoke neuronal responses (Arabzadeh et al., 2005; Wolfe et al., 2008; Jadhav et al., 2009), but whisking against a smooth surface such as a metal pole generally elicits only weak dynamic effects at the whisker base (Quist et al., 2014).

For whisking against smooth objects, a whisker's shape can, aside from occasional slips, be approximated as a continuously changing steady state, where the shape at any given time depends on the applied force at that time. This 'quasi-static' case is not universally applicable but, as detailed in the next section, it is the basis for a mechanically rooted experimental paradigm that has given substantial novel insight into somatosensation. Unless stated to the contrary, the following discussion assumes the quasi-static case.

Forces at the whisker base

Suppose a time-independent force is applied to a whisker. Such a force exerts a rotatory effect on the whisker ('moment'), which makes it bend around a pivot near its base. In steady state, the applied force and the moment are balanced by reaction force and reaction moment at the whisker base. In general, both the forces and moments are 3D, implying a total of 6 mechanical variables acting at the whisker base. However, 3D forces/moments are challenging to estimate (for progress, see Huet et al., 2015; Loft et al., 2016) and almost all studies to date have considered experimental conditions where whisker motion and whisker forces/moments are predominantly planar. Whisking motion occurs largely, but not entirely, in the horizontal plane defined by the two eyes and the nose (Bermejo et al., 2002; Knutsen et al., 2008). Thus, when a rat/mouse whisks against a vertical surface, such as a pole, whisker–object contact force and whisker bending is largely in the horizontal plane: these effects can be measured by imaging in this plane. In this 2D case, whisker–object contact is characterized by 3 mechanical variables at the whisker base: a 2-component applied force $\vec{F}$ directed at some angle in the horizontal plane and a moment M_0 directed about the vertical axis through the whisker base, normal to the horizontal plane (see Fig. 1).

It is important to define $\vec{F}$ so that its relationship with mechanoreceptor activity is as direct as possible. Since mechanoreceptors are embedded in the whisker follicle, and since the follicle rotates rigidly during whisking (Bagdasarian et al., 2013), the natural coordinate system is a ''whisker-centric" one (Pammer et al., 2013; Hartmann, 2015). The coordinate axes are 'axial' (pushing whisker into its follicle) and 'lateral' (pushing the whisker at 90 degrees to the follicle); the origin is at the base of the whisker (Fig. 1). In whisker-centric coordinates, $\vec{F}$ is

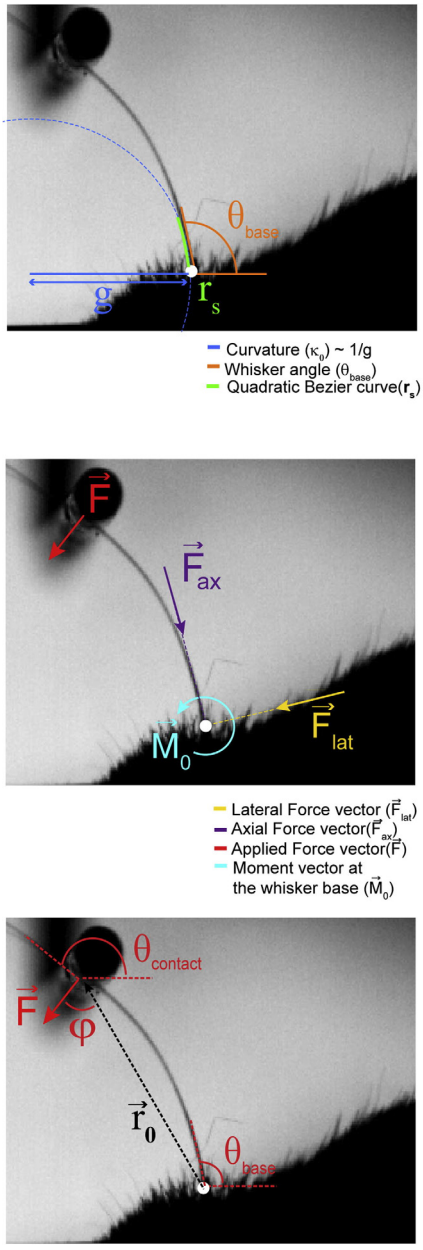

Notation:

$\mathbf{r}_s = [x_s, y_s]$: quadratic Bezier curve fitted to the basal section of the whisker, where s parameterises location along the curve; $s = 0$ at the whisker base.

Definition of whisker curvature:

$$\kappa_s = \frac{x_s' y_s'' - x_s'' y_s'}{(x_s'^2 + y_s'^2)^{3/2}}$$

where x, y are horizontal/vertical coordinates of the image, x_s', y_s' and x_s'', y_s'' are the *1st* and *2nd* derivatives of the functions x_s and y_s with respect to s.

Notation:

M_0 : bending moment about the vertical axis through the whisker base ($s = 0$).

$\vec{F}$: applied force of object against whisker at the contact point.

F_{ax} F_{lat} : axial and lateral components of $\vec{F}$ (whisker-centric coordinates).

Definition of applied force and moment:

$$M_0 = F\, r_0\, sin(\varphi)$$

where r_0 and F are length of the "lever arm" vector ($\vec{r_0}$) connecting the whisker base to the contact point and magnitude of the applied force vector ($\vec{F}$) respectively.

$$F_{ax} = F\, sin(\theta_{base} - \theta_{contact})$$

$$F_{lat} = F\, cos(\theta_{base} - \theta_{contact})$$

where θ_{base} and $\theta_{contact}$ are respectively the angle between the tangent to the whisker at its base and the horizontal, and the angle between the tangent to the whisker at the contact point and the horizontal.

Fig. 1. Forces at the whisker base and their measurement. Whisker angle (θ), bending moment at the whisker base, (M_0), applied force ($\vec{F}$) and its component axial force (F_{ax}) and lateral force (F_{lat}) can be measured during active whisker object interaction, by filming the whisker at high speed and processing each frame using a whisker-tracking algorithm. In this example, a quadratic Bezier curve (r_s) is fitted to the segment of the whisker near its base. Whisker angle is defined as the angle between the tangent to r_s at the whisker base ($s = 0$) and the horizontal. Whisker curvature (κ_s) is computed from the Bezier quadratic fitting using the equation and is proportional to the reciprocal of the radius of the circle (g) which best fits the Bezier curve at point s (blue dotted line). (Adapted from Campagner et al., 2016).

thus expressed in terms of an axial component F_{ax} and a lateral one F_{lat}.

While restricting analysis to the horizontal plane is experimentally advantageous, there are caveats. First, any vertical component of whisker motion (Knutsen et al., 2008) and any vertical component of bending (Huet et al., 2015) will be missed. Second, since whiskers are intrinsically curved and rotate about the axis of the follicle during whisking (Knutsen et al., 2008), imaging in the horizontal plane can register apparent changes in whisker shape that may be confused with bending. Third, any moment (torque) about the follicle axis will be missed (Huet et al., 2015). In 3D whisker-centric coordinates, the applied force has 1 axial component and 2 lateral components, the moment has 2 components of bending and 1 of torsion/roll about the long axis of the follicle (Huet et al., 2015).

ESTIMATION OF MECHANICAL WHISKER VARIABLES

One of the drivers of recent progress has been the development of techniques for measuring these whisker mechanical variables experimentally in the awake, behaving animal. In this section, we outline the theoretical foundation.

Consider a whisker that is being bent due to contact with an object such as a pole. Whiskers are intrinsically curved: contact changes the whisker's curvature with respect to its intrinsic (undeformed) value. As noted above, in steady state, there is a simple relationship between the bending moment (M_p) about a point p (located along the whisker shaft between the whisker base and the contact point) and the curvature κ_p of the whisker at that point (Birdwell et al., 2007). The fundamental equation is:

$$M_p(t) = \Delta k_p(t) E_p I_p \qquad (1)$$

Here $\Delta k_p(t)$ is the change in the whisker's curvature compared to its intrinsic shape at time t and $E_p I_p$ is a constant of proportionality ('bending stiffness'). (From this point on, to reduce clutter, the t dependence is omitted). The equation states simply that, the stiffer a whisker, the greater the moment implied by a given change in curvature. The constant consists of a factor E_p ('Young's modulus') that depends only on the material composition of the whisker and a factor I_p ('area moment of inertia') that depends only on the geometry of the whisker. E_p has typical values of 2-5GPa (Hartmann, 2015), but may vary somewhat across whiskers and with p (Quist et al., 2011). I_p depends only on the cross-sectional area of the whisker at the point p and, for an object with circular cross-section, $I_p = \frac{\pi}{4} a_p^4$, where a_p is the radius of the whisker at point p. Because I_p depends on the fourth power of the radius, the variation

in stiffness along the whisker shaft is dramatic: for a typical whisker whose tip diameter is 10% of its base diameter, bending stiffness at the base is 10,000 times greater at the base than at the tip.

Eq. (1) is of fundamental, practical importance, since it indicates that mechanical variables associated with whisker touch can be estimated in an experimentally feasible manner by imaging a whisker's shape. The simplest approach is to estimate the curvature change at the whisker base Δk_0 (Fig. 1). Provided that, during the course of a video, Δk_0 is measured at the same point ($p = 0$) along the whisker shaft (so that the bending stiffness is constant) this measure is proportional to M_0. A second approach is possible if measurements of a_0 and E_0 are also available: in this case, I_0 can be calculated and thereby M_0 itself. However, since whiskers can grow over the time-course of a typical behavioral experiment (Ibrahim and Wright, 1975), and since the bending stiffness is sensitive to radius (a 10% change in a_0 changes I_0 by 46%), estimates of M_0 are more delicate. With both approaches, care must be taken to ensure that the location at which the curvature is measured is constant and as close as possible to the whisker base. An alternative, more complex, approach is to model a whisker as a series of links connected by torsional springs and fit its parameters to imaging data (Quist et al., 2014).

To complete the description of the forces acting on the whisker base, it is necessary to estimate the applied force $\vec{F}$ (Pammer et al., 2013). The principle here is that a force applied to some point on a whisker exerts a moment M_0, which is the product of the force magnitude and distance between the whisker base and the line of action of the force. Thus, if this distance can be measured, the force magnitude can be obtained by working backward from an estimate of M_0. An equivalent, and experimentally useful, form of this expression for M_0 is:

$$M_0 = F r_0 \sin(\varphi) \tag{2}$$

Here F is the magnitude of $\vec{F}$, r_0 is the length of the lever arm vector $\vec{r}_0$ that connects the base of the whisker to the contact point and φ is the angle between $\vec{F}$ and $\vec{r}_0$ (see Fig. 1). The equation expresses the fact that, to open a door, it is more effective to push in a direction normal to it ($|\varphi| = 90°$, $|\sin(\varphi)| = 1$) than at an angle ($|\varphi| < 90°$, $|\sin(\varphi)| < 1$) and more effective to situate the handle near the edge (large r_0) than near the hinge (small r_0). To obtain values for F_{ax} and F_{lat}, it is necessary to know the direction of $\vec{F}$. If friction can be approximated as zero, this direction is normal to the whisker at the contact point (Fig. 1) and:

$$F_{ax} = F \sin(\theta_{base} - \theta_{contact}) \tag{3}$$

$$F_{lat} = F \cos(\theta_{base} - \theta_{contact}) \tag{4}$$

Here θ_{base} and $\theta_{contact}$ are angles that define the geometry of the contact (Fig. 1). These quantities can be estimated from images of the whisker. Procedures to take account of friction have been proposed and, for whisking against smooth, metal poles, have little effect on the frictionless force estimates (Pammer et al., 2013; Hires et al., 2016; Huet and Hartmann, 2016).

Whisker imaging and tracking

Qualitative "cinematographic" analysis of whisking was first done by Welker (1964). However, to put the above theory into practice, it is necessary to obtain quantitative kinematic/mechanical information from individual video frames. In the first study to quantify whisker motion, the angle of whiskers to the head ('whisker angle') was measured by putting a transparency over the video monitor and tracing whiskers on to it by hand (Carvell and Simons, 1990). Later studies developed a variety of semi-automated techniques for measuring whisker kinematics (i.e., whisker angle) based on beam-break sensors (Bermejo et al., 1998, 2002; Arabzadeh et al., 2005; Wolfe et al., 2008; Jadhav et al., 2009; Khatri and Bermejo, 2009), computer-assisted, manual tracking (Grant et al., 2009), tracking the location of spots of dye (Knutsen et al., 2008; Venkatraman et al., 2009; Nashaat et al., 2017; Rigosa et al., 2017) and segmentation of whiskers from video (Ritt et al., 2008; Voigts et al., 2008; Perkon et al., 2011).

To estimate the key mechanical variables defined above, it is necessary to track not just whisker kinematics but also whisker curvature. This has required machine vision techniques that extract the shape of one or more whiskers from imaging data (Knutsen et al., 2005; O'Connor et al., 2010a; Clack et al., 2012; Pammer et al., 2013; Bale et al., 2015a; Campagner et al., 2016). Application of machine vision has also made it feasible to measure whisker motion from high-speed video (~1000 frame/s) on large data sets. For example, one recent study (Campagner et al., 2016) involved quantification of ~1.5 million video frames.

With these methods, the shape of a whisker is captured by fitting a parametric curve $\boldsymbol{r}_s = [x_s, y_s]$ to the image of a whisker (where s indicates location along the whisker; Fig. 1). In principle, it is then straightforward to calculate the required curvature κ_s defined in Fig. 1.

However, κ_s depends on second derivatives of x_s and y_s, which are sensitive to estimation error. In order to obtain good-quality curvature estimates, care is necessary to ensure that the whisker images are high quality and that the curve $\boldsymbol{r}_s$ is fitted as accurately as possible. The challenges here are that the whisker tip is hard to image since it is small, moves rapidly and can move out of the focal plane. Also, the complete shape of a whisker in contact with an object can be complex: many free parameters are required to describe a complex curve and this again increases estimation error. As noted above, it is forces at the base of the whisker that are most closely related to mechanotransduction. Thus, recent studies have focussed on estimation of the curvature near the base. The basal part of a whisker is most readily imaged (radius is comparatively large, moves most slowly and least out of the focal plane) and is well-approximated by a quadratic function (Quist and Hartmann, 2012; Pammer et al., 2013) which (in 2D) has only 6 free parameters. The basal part can either be described by refitting a quadratic function to this portion of the complete, tracked whisker (Clack et al., 2012; Pammer et al., 2013) or by restricting whisker tracking to the basal section of the

whisker (Bale et al., 2015a; Campagner et al., 2016). Whisker–object contact parameters, which are required in order to estimate F_{ax} and F_{lat}, can be measured by tracking the segment of whisker near the contact point.

Two approaches to such tracking have been developed. One approach is to analyze each frame independently. This has the important advantage of speed, since multiple frames can be tracked in parallel (Clack et al., 2012). However, temporal information is useful for making whisker tracking more robust in the face of complexities such as whisker overlap (Bale et al., 2015a), although at the cost of reduced tracking speed.

To summarize the above discussion, the following equations describe how the bending moment at whisker base (M_0), and the applied force (magnitude F, components F_{ax} and F_{lat}) can be estimated from whisker-tracking outputs ($\Delta\kappa_0$, r_0, θ_{base}, $\theta_{contact}$ and φ) along with whisker radius (a_0) and Young's modulus (E_0):

$$M_0 = \frac{\pi}{4} a_0^4 \Delta\kappa_0 E_0 \tag{5}$$

$$F = \frac{\pi}{4} \frac{a_0^4 \Delta\kappa_0 E_0}{r_0 \sin(\varphi)} \tag{6}$$

$$F_{ax} = \frac{\pi}{4} \frac{a_0^4 \Delta\kappa_0 E_0}{r_0 \sin(\varphi)} sin(\theta_{base} - \theta_{contact}) \tag{7}$$

$$F_{lat} = \frac{\pi}{4} \frac{a_0^4 \Delta\kappa_0 E_0}{r_0 \sin(\varphi)} cos(\theta_{base} - \theta_{contact}) \tag{8}$$

As noted above, these equations apply to experiments designed so that the forces/moments act in the horizontal plane. Ideally, however, one would like to be able to estimate the complete set of the six mechanical variables, which describes the complete mechanical state of the whisker base in 3D. Whisker kinematics have been tracked in 3D (Bermejo et al., 2002; Arabzadeh et al., 2005; Knutsen et al., 2008), but mechanical analysis requires tracking the full whisker shape, which, although there has been progress, poses on-going challenges (Huet et al., 2015; Loft et al., 2016).

ENCODING OF MECHANICAL SIGNALS IN PRIMARY WHISKER AFFERENTS

Numerous studies, employing diverse experimental paradigms, have sought to investigate how physical signals associated with touch drive the responses of neurons in the whisker system. The bulk of these studies have focused on the relationship between kinematic variables (whisker position, velocity etc) and neuronal activity. However, as discussed above, ultimately, it is mechanical forces/moments acting on the whisker base that drive mechanotransduction. Until recently, the relationship between whisker kinematics and mechanical variables (forces, moments, and proxies to them) was unknown. Hence it was unclear what mechanical variables, are actually encoded. Recently, however, recordings of neuronal activity have been made simultaneously with direct estimation of mechanical variables using the approach reviewed above. This has resulted in substantial new insight into the mechanical basis of neural coding in the whisker system. Our primary focus here is on neural coding at the first level of the system – the primary whisker afferents (PWAs).

Passive stimulation

In the 'passive stimulation' paradigm (Zucker and Welker, 1969; Gibson and Welker, 1983), whisker movement is suppressed by global anesthesia and sensory stimulation applied by deflecting the whiskers, typically by means of mechanical actuators. Passive stimulation is useful to investigate questions for which a high degree of experimental control of the sensory input is essential. Such experiments have provided fundamental insight into the functional architecture of barrel cortex (Simons, 1978; Armstrong-James and Fox, 1987; Petersen and Diamond, 2000; Petersen et al., 2003), experience-dependent plasticity (Armstrong-James et al., 1992) and adaptation (Maravall et al., 2007, 2013; Wang et al., 2010). Studies have also shown that neurons in the whisker system are capable of firing spikes timed with sub-millisecond precision (Petersen et al., 2001; Panzeri et al., 2001; Arabzadeh et al., 2005; Montemurro et al., 2007; Bale and Petersen, 2009). A recent study showed, by high sampling rate electrophysiological recording (500 kHz), that the physical limits of spike timing precision are at the microsecond scale: spike timing jitter in PWAs in response to rapid whisker deflection was on average 17.4 μs with the most precise neurons exhibiting jitter of 5.1 μs (Bale et al., 2015a).

Passive stimulation experiments have also provided much data concerning the relationship between whisker kinematics and PWA activity (Zucker and Welker, 1969; Gibson and Welker, 1983; Lichtenstein et al., 1990; Shoykhet et al., 2000; Jones et al., 2004; Leiser and Moxon, 2006; Kwegyir-Afful et al., 2008; Bale and Petersen, 2009; Storchi et al., 2012; Bale et al., 2013; Maravall et al., 2013). It has, however, been unclear what mechanical variables drive PWA responses under these conditions. In a typical experiment, the whisker is trimmed to a length of a few mm and the whisker stump is deflected laterally by an actuator. According to the mechanical framework discussed above, the actuator applies a force on the whisker shaft, which exerts a moment that makes the whisker bend. However, in a typical passive stimulation experiment, the whisker appears to rotate as a rigid body; no bending is typically apparent (at least by eye). One possibility is that the theory makes some assumption that fails to generalize *in vivo*. However, another possibility is suggested by considering the mechanics of the experiment. Trimming results in a short whisker stump. Since whiskers are tapered, the stump is the thickest, and stiffest, part of a whisker. Equation (1) therefore implies that there may be an appreciable bending moment, but that the associated change in curvature of the stump is slight due to its stiffness. To test between these possibilities, Campagner et al. (2016) used high-

speed imaging to measure how the shape of a whisker stump changes during passive stimulation. They measured small but reliable changes in whisker curvature during stimulation and, by varying the magnitude of the deflection, showed that bending correlates linearly with deflection angle (correlation coefficient ~0.95). This confirms that passive deflection does bend a whisker in vivo, as predicted by the mechanical theory. The significance of these findings is the implication that, under typical passive stimulation conditions, there is a simple relationship between kinematic and mechanical whisker variables: whisker deflection angle is proportional to bending moment M_0.

This relationship allows kinematic tuning results from passive stimulation studies to be reinterpreted within the whisker mechanical framework. PWAs have been reported to be tuned to the direction of deflection (in the plane normal to the whisker shaft, Gibson and Welker, 1983; Lichtenstein et al., 1990; Bale and Petersen, 2009). Some PWAs are tuned to the amplitude of deflection, some to the velocity of deflection but most are tuned to a weighted sum of amplitude and velocity, with different neurons having different weightings (Shoykhet et al., 2000; Kwegyir-Afful et al., 2008; Bale et al., 2013). Using the observation of Campagner et al. (2016) that deflection angle is proportional to M_0, which also implies that deflection velocity is proportional to $\dot{M}_0$ (the temporal derivative of M_0), the implication is that PWAs are tuned to the direction of bending within the lateral plane and that PWAs are sensitive to a weighted sum of M_0 and $\dot{M}_0$. This interpretation is corroborated by a subsequent study which found that PWA responses to passive deflection of whiskers are well-predicted by the time series of M_0 (Bush et al., 2016). There is evidence that some PWAs respond to deflection in the axial direction (Stüttgen et al., 2008): the results are suggestive of tuning to axial force but, since whisker shape was not measured in this study, bending may have contributed to the responses. In summary, the framework of whisker mechanics can account for many results from passive stimulation by the hypothesis that PWAs encode moment and its temporal derivative.

Artificial whisking

In the 'artificial whisking' paradigm (Zucker and Welker, 1969; Szwed et al., 2003, 2006; Arabzadeh et al., 2005; Lottem and Azouz, 2011; Wallach et al., 2016), whisker movement is produced by dissecting out the buccal motor branch of the facial nerve and electrically stimulating it, in an anesthetized animal. Sensory stimulation is produced by positioning objects in the path of the whiskers. Artificial whisking (Zucker and Welker, 1969; Szwed et al., 2003) is useful since whisker–object contact forces are produced in a fashion that mimics the active character of awake, whisking behavior, but can be controlled and repeated by the experimenter. The paradigm differs from natural whisking in that both intrinsic and extrinsic muscles are excited in phase (Szwed et al., 2006).

Artificial whisking studies led to the first descriptions of how active whisker–object contact and whisking phase might affect PWA activity. Three neuronal subtypes have been reported: whisking neurons, touch neurons and whisking-touch neurons. Whisking neurons fire at specific phases of the whisker cycle (Szwed et al., 2003, 2006; Wallach et al., 2016) and their response is invariant to weak whisker–object contact. Touch neurons fire only during contact and are subdivided into pressure neurons (fire for the entire duration of contact), contact neurons (fire only at onset of contact), detach neurons (fire only at offset of contact) and contact-detach neurons (fire at both onset and offset of contact). Whisking-touch neurons fire both during whisking (in a phase-locked fashion) and in response to contact (Szwed et al., 2003, 2006). For most touch-sensitive PWAs, firing rate depends on radial pole location, decreasing with distance of contact from the face (Szwed et al., 2006).

How might these artificial whisking data be explained by the whisker mechanics? Since modeling suggests whisker forces to be substantially weaker during whisking in air compared to contact (Quist et al., 2014), some of the diversity in neuron types can be accounted for by the empirical observation that PWAs differ in their response threshold (Zucker and Welker, 1969). Neurons with low deflection thresholds would be expected to respond to both whisking and touch; neurons with higher threshold only to touch. A possible mechanical basis of whisking neurons is discussed below. Responses to whisker–object contact can be accounted for by the hypothesis that PWAs encode M_0 in the following way (Birdwell et al., 2007). A neuron sensitive to M_0 should respond to touch, since touch causes bending. Diversity in touch responses can be accounted for by variation in the extent to which neurons weight M_0 compared to $\dot{M}_0$. Neurons with high weighting to M_0 would be expected to respond throughout contact (pressure type). Neurons with high weighting to $\dot{M}_0$ would be expected to respond primarily to contact onset or offset, depending on the directionality of their sensitivity. Due to the marked variation in stiffness along the shaft of a tapered whisker, the M_0 produced by a given contact is much weaker for contact on a distal part of the whisker compared to a proximal part. Thus neurons sensitive to M_0 would be expected to fire at a higher rate to proximal compared to distal contacts. In summary, how PWAs respond to whisker–object contact during artificial whisking can be accounted for in a straightforward way by moment coding.

Awake, behaving conditions

In any sensory system, a major challenge is to understand the principles of sensory coding to the point that the activity of primary afferents can be accurately predicted in the awake, behaving animal. In the whisker system, the cell bodies of the primary afferents are located in the trigeminal ganglion. This ganglion is awkwardly located for the electrophysiologist, at the base of the skull, and awkwardly organized, with low neuronal density and lack of clear somatotopy (Leiser and Moxon, 2006). These features compound the usual challenges of recording from awake, behaving animals. Two pioneering studies first succeeded in recording PWA activity from awake, behaving rats (Leiser and Moxon, 2007; Khatri and Bermejo, 2009), but were limited

by the whisker-tracking tools available at the time. Recent studies, using new tools and building on the mechanical approach outlined above, have succeeded in identifying mechanical predictors of PWA activity in the awake, behaving animal. The first of these studies was by Campagner et al. (2016), with subsequent work by Bush et al. (2016) and Severson et al. (2017).

Progress in high-speed imaging and whisker tracking has led to a new generation of studies which have succeeded in measuring neuronal activity from subcortical and cortical regions of the whisker system, while, at the same time, measuring whisker mechanical/kinematic variables at millisecond resolution (O'Connor et al., 2010b, 2013; Huber et al., 2012; Petreanu et al., 2012; Xu et al., 2012; Peron et al., 2015; Bush et al., 2016; Campagner et al., 2016; Severson et al., 2017). In most studies to date, high-speed cameras (500–1000 frames/s) have been used to record whisker movements in head-restrained mice, as they whisk either in air or against an object. As discussed above, a whisker-tracking algorithm is then used to extract whisker kinematic variables and whisker shape variables from each frame, resulting in time series that describe the mouse's whisking behavior and the whisker–object interaction. From these data, mechanical variables ($\vec{F}$ and M_0) or proxies to them ($\Delta\kappa_0$) are calculated.

In contrast to the passive stimulation paradigm, sensory variables cannot be closely controlled, since the animal is awake and behaving, but they can be measured and a statistical model, such as a Generalized Linear Model (GLM), can be used to attempt to predict a PWA's spike train based on one or more whisker mechanical/kinematic variables (Campagner et al., 2016). However, an important, and widely applicable caveat is that sensory variables measured from awake animals typically have awkward statistical properties (correlations over both variables and time). For example, whisker angle correlates with whisker bending (Campagner et al., 2016). Thus, in a traditional tuning curve analysis, a neuron that is tuned purely to bending might appear also to be tuned to angle, simply as an artifact of the correlation. Multiple Regression and extensions to it, such as GLM, can handle correlation, provided it is not too strong. However, beyond a certain correlation strength ('multicollinearity'), it becomes impossible to tease the influence of different sensory variables apart, and results can be misleading, particularly if the data sample is small (Wooldridge, 2012). It is therefore important to use an experimental design that, as far as possible, decouples sensory variables of interest. In the studies of PWAs in awake animals that are the main focus here, this has been achieved by varying the spatial location of the object that the animal whisks against from trial to trial (Campagner et al., 2016; Severson et al., 2017).

Whisking in air. Most PWAs fire at a higher rate during whisking than when the whiskers are still, and some PWAs, particularly those with high firing rate during whisking, show phase-locked responses (Leiser and Moxon, 2007; Khatri et al., 2009; Campagner et al., 2016; Severson et al., 2017; Fig. 2B). What might be the mechanical basis of this activity? Whiskers are controlled by intrinsic and extrinsic muscles (Berg and Kleinfeld, 2003). To make a whisker move, the muscle force must overcome resistance from both the mass of the whisker (inertial force) and the springiness/viscosity of mystacial pad tissue (viscoelastic force). In principle, any of these forces, alone or in combination, could drive follicular mechanoreceptors. We consider first the inertial force. Due to taper, the 70% or so of a whisker closest to the base is relatively stiff and moves as a rigid object during whisking (Quist et al., 2014). Hence its angular acceleration is expected to be proportional to moment (torque) (Quist et al., 2014). The hallmark of a moment-sensitive neuron is therefore that its firing rate should increase with angular whisker acceleration. Consistent with this, the firing rate of some PWAs can be predicted, during free whisking, from angular whisker acceleration (Campagner et al., 2016; Severson et al., 2017; Fig. 2C). Since acceleration varies during the whisking cycle (the precise phase relationship depending on the exact waveform of the cycle), moment coding can potentially explain phase selectivity of PWAs: indeed, for some PWAs, phase tuning can be predicted from acceleration (Severson et al., 2017) Since it takes more acceleration to move a whisker with greater amplitude and greater frequency, moment coding can also explain correlation between PWA firing rate and both whisking amplitude (Khatri et al., 2009) and whisking frequency (Leiser and Moxon, 2007). Phase tuning can be predicted with increased accuracy using a multivariate model that includes both acceleration and other kinematic variables as inputs (Severson et al., 2017): this may reflect influence of viscoelastic forces on the mechanoreceptors.

An elegant test of whether PWAs are sensitive to inertial moment is based on the fact that, if the mass of a whisker is changed, the firing rate of an inertia-sensitive neuron, at a given angular acceleration, should change correspondingly (Severson et al., 2017). This prediction was confirmed by progressive trimming of the whiskers in a subset of PWAs. Because of the low mass of whiskers (of order 10–100 μg) and, due to taper, the concentration of this mass near the base, moment at the whisker base – as inferred by modeling – is likely to be orders of magnitude smaller than those generated by whisker–object contact (Quist et al., 2014). This suggests that at least some whisker mechanoreceptors are exquisitely sensitive.

However, the response of PWAs to whisking in air cannot be entirely explained by sensitivity to inertial moment. Some PWAs do not change firing rate after whisker trimming (Severson et al., 2017) and the activity of a minority of whisking-sensitive PWAs cannot be well-predicted by angular acceleration (Campagner et al., 2016; Fig. 2C). Moreover, some brainstem/thalamic neurons, with receptive fields on the microvibrissae or fur around the mouse/nose, exhibit activity that is modulated by the whisking rhythm (Moore et al., 2015). Although it cannot be excluded that these neurons are driven by inertial moment, the very low inertia of such very short, very light hairs, renders this unlikely. What might be driving the activity of the non-inertia coding PWAs? Severson

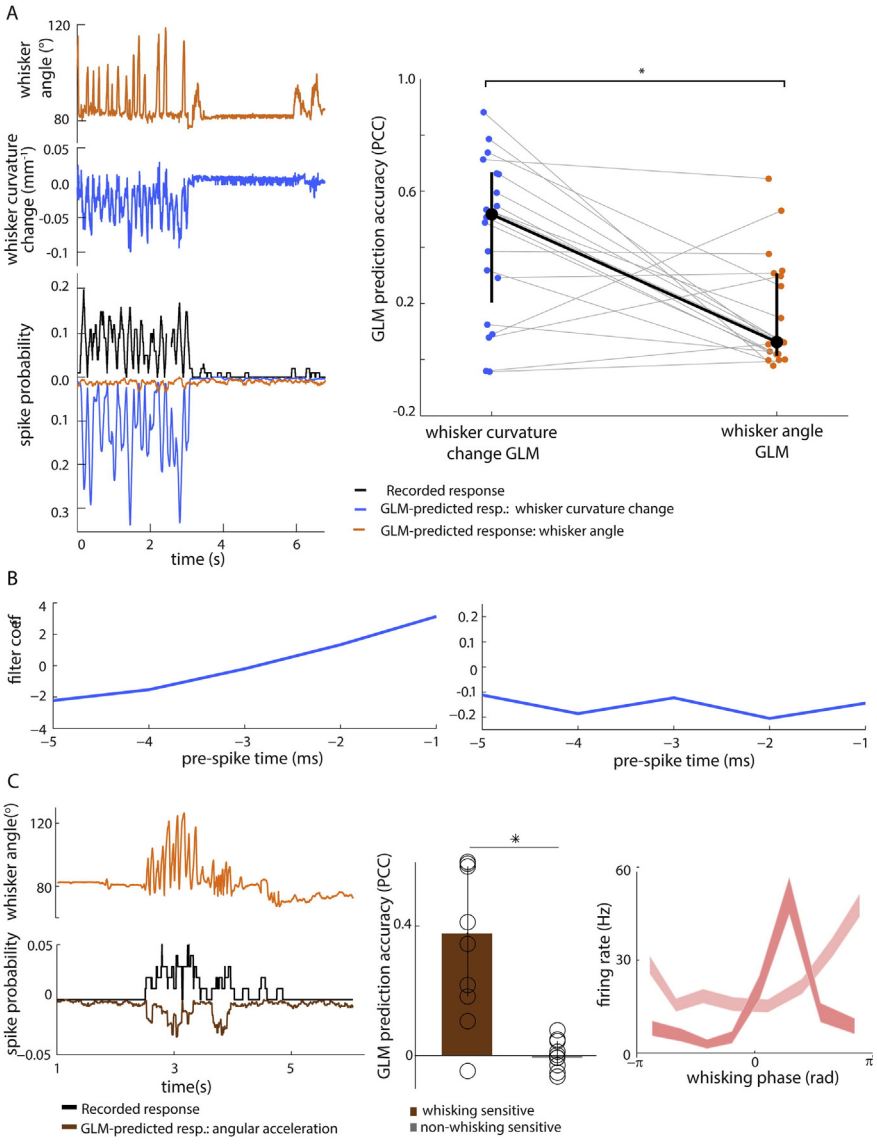

Fig. 2. PWA activity predicted by mechanical/kinematic variables in awake, behaving mice. Mice whisked against a pole, while the activity of PWAs was recorded at the same time as whiskers were imaged at 1000 frames/s (Campagner et al., 2016). A. PWAs encode curvature change, not whisker angle. *Left:* Example of whisker angle (top panel) and whisker curvature change (used as a proxy for moment top panel) and simultaneously recorded smoothed spike train of a PWA (bottom panel, black), together with predicted spike trains for the best-fitting angle GLM (bottom panel, orange) and curvature-based GLM (bottom panel). *Right:* Model prediction accuracy was computed by calculating a cross-validated Pearson correlation coefficient between the real and predicted spike trains. For each PWA, model prediction accuracy is shown for both angle-based and curvature-based GLMs (black dots median; error bars interquartile range; * indicates signed ranked test, p = 0.0044). B. Stimulus filter of curvature change GLMs for two PWAs. The stimulus filter of unit on the right was negative (in the 5 ms preceding a spike), indicating sensitivity to negative curvature change. The stimulus filter of unit on the left was biphasic, but with positive integral, indicating sensitivity both to positive curvature change and to positive curvature change derivative. C. PWAs encode moment during in air whisking. Left: Excerpt of whisking in air along with activity of an example, whisking-sensitive PWA and activity predicted by a GLM driven by angular acceleration. Whisking-sensitive PWAs were defined as ones whose firing rate significantly correlate with whisking amplitude. Middle: Prediction accuracy of acceleration-based GLMs for whisking-sensitive and non-whisking-sensitive PWAs (* indicates $p = 0.0017$, ranksum test). Right: Tuning curves to whisking phase for two example whisking-sensitive PWAs.

et al. (2017) found that PWAs whose firing rates were unaffected by whisker trimming were phase-locked to the EMG of either intrinsic or extrinsic muscles. Collectively, these results indicate that activity of PWAs during whisking in air can largely be explained by sensitivity to either inertial moment or muscle contraction force.

Although studies of artificial whisking have reported a substantial number of 'whisking neurons' (Szwed et al., 2003), studies of awake mice have found neurons sensitive to whisking but not touch to be rare (Campagner et al., 2016; Severson et al., 2017). The reasons for this discrepancy are unclear, but note that, in artificial whisking studies, a 'whisking neuron' is defined as a neuron that is insensitive to weak contact (Knutsen and Ahissar, 2009; Wallach et al., 2017). In the awake animal, where both weak and strong contacts occur, such a neuron might be classified as sensitive to both whisking and touch. A tentative mechanical explanation for whisking neurons is that they might be responsive not only to muscular contraction (Severson et al., 2017), but also to bending moment with high threshold (thereby responding only to strong contacts).

Whisker–object contact. PWAs fire at a higher rate during whisker–object contact than during whisking (Leiser and Moxon, 2007; Campagner et al., 2016; Severson et al., 2017). The major finding from awake animals is that PWA firing rate can be predicted, using statistical models, from time series of either M_0 or its proxy $\Delta\kappa_0$ (Campagner et al., 2016; Bush et al., 2016; Severson et al., 2017; Fig. 2A). There is consistent evidence, from the temporal profile of GLM parameters (Campagner et al., 2016; Fig. 2B) and from prediction accuracy (Severson et al., 2017) for coding of both M_0 and its temporal derivative $\dot{M}_0$. The relative importance of M_0 and $\dot{M}_0$ for predicting activity varies from neuron to neuron, and is likely to depend on the extent to which rapid bending changes occur during the conditions of a particular recording. Although F_{ax} and F_{lat} predict PWA activity less accurately, on average (Campagner et al., 2016; Severson et al., 2017), adding F_{ax} or F_{lat} as model inputs alongside M_0 improves prediction for a minority of neurons and, for a few PWAs, F_{ax} or F_{lat} are better predictors than M_0 (Bush et al., 2016; Campagner et al., 2016; Severson et al., 2017).

An apparent discrepancy between studies of awake animals concerns how well PWA activity can be predicted from kinematics. Campagner et al. (2016) reported that mechanical variables predict PWA activity better than kinematic ones, whereas Bush et al. reported no difference. One potential source of discrepancy is that the studies quantified kinematics differently. However, discrepancy remains even when comparing results where kinematics were measured in a similar way (as θ_{push} – the change in angle of whisker to head during an episode of whisker–object touch). Instead, an important factor is likely to be the degree to which mechanical and kinematic variables were correlated in the conditions of the two studies. Bush et al. (their awake recordings) used experimental conditions where θ_{push} was tightly coupled to M_0. In contrast Campagner et al. (2016) decoupled the variables by varying rostro-caudal object location and were therefore able to tease the roles of the variables apart, finding greater predictive power for mechanical variables compared to kinematic ones. Consistent with this account, when Bush et al. (2016) decoupled the variables under anesthetized conditions, they also found greater predictive power for mechanical variables.

In summary, the results of this section suggest the major variable that PWAs encode is M_0, but also that there is functional diversity in the PWA population (Bale et al., 2013).

Diversity of PWA function and its anatomical basis

The discovery of genetic markers for different mechanoreceptors, together with development of intra-axonal recordings and optogenetic tagging methods, is starting to permit dissection of the anatomical basis of this diversity (Tonomura et al., 2015; Severson et al., 2017; Takatoh et al., 2017). In an important advance, Severson et al. (2017) optically tagged Merkel cell PWAs, and demonstrated that they were tuned to a combination of M_0 and $\dot{M}_0$ Why might different PWAs encode different mechanical variables? The whisker follicle is a heterogeneous structure composed of distinct cell layers, differing in their density and viscoelastic properties. The follicle contains several morphologically distinct classes of mechanoreceptive nerve ending (Merkel cell-neurites, lanceolate, reticular, club-like, Ruffini-like and free nerve endings), which are located in different cell layers and/or at different depths within the follicle (Rice and Munger, 1986; Rice et al., 1993; Ebara et al., 2002; Sakurai et al., 2013; Tonomura et al., 2015). It has been suggested that mechanoreceptive nerve endings detect strain in the tissue within which they are embedded (Mitchinson et al., 2004; Lottem and Azouz, 2011; Severson et al., 2017). If follicle tissue behaves like a spring, this strain will reflect M_0; if, instead, it behaves like a damper (viscosity), strain will reflect $\dot{M}_0$. In the actual follicle, different cell layers are likely to differ in their mechanical properties, indicating that functional heterogeneity may be a consequence of nerve endings being embedded in different locations within the follicle (Mitchinson et al., 2004). Spring–damper models can account both for whisker–object contact responses recorded by artificial whisking (Mitchinson et al., 2004) and for activity recorded in awake, behaving animals (Severson et al., 2017). This suggestion for the origin of PWA heterogeneity is supported by a recent report that whisker deflection produces a gradient of strain through the follicle (Whiteley et al., 2015). PWA encoding may also be influenced by biophysical differences between classes of mechanoreceptive nerve ending (Mitchinson et al., 2004; Tonomura et al., 2015; Severson et al., 2017).

TRANSFORMATIONS IN MECHANICAL CODING ACROSS THE ASCENDING SOMATOSENSORY PATHWAY

Part of the significance of the progress in understanding what the primary afferents tell the brain is that it provides a baseline for understanding how downstream circuits transform the ascending drive, and use it as the basis for behaviorally oriented computations. In this section, therefore, we compare how mechanical signals are encoded in the periphery to how they are encoded in cortex (see also Bale and Maravall, 2018).

In one respect, encoding in cortex and periphery are similar. Studies of both barrel cortex and motor cortex have shown widespread encoding of whisker base curvature – and therefore of M_0 (O'Connor et al., 2010b, 2013; Huber et al., 2012; Petreanu et al., 2012; Chen et al., 2013; Yu et al., 2016). Although no study has yet directly tested for $\dot{M}_0$ tuning in cortex, there is indirect evidence. First, layer 4 neurons exhibit a robust, transient response to touch (Hires et al., 2015): since touch involves sudden onset of whisker bending, and hence high, transient $\dot{M}_0$, this response is likely to correlate better with $\dot{M}_0$ than M_0. Second, passive stimulation studies have consistently shown, in anesthetized animals, that cortical neurons encode the velocity of deflection angle (Pinto et al., 2000; Arabzadeh et al., 2003; Maravall et al., 2007; Estebanez et al., 2012). As discussed above, since deflection angle correlates tightly with whisker bending under passive stimulation conditions (Campagner et al., 2016), this is consistent with cortical encoding of $\dot{M}_0$. Collectively, these data indicate that information about bending moment is preserved across the ascending pathway, suggesting that M_0 and $\dot{M}_0$ are important mechanical variables underlying touch-based behavior.

In another respect, encoding in cortex is markedly different to that in the periphery. Studies of actively sensing animals demonstrate that whisking elicits robust 'self-motion' activity in PWAs, even in the absence of touch (Szwed et al., 2003, 2006; Leiser and Moxon, 2007; Khatri and Bermejo, 2009; Campagner et al., 2016; Wallach et al., 2016; Severson et al., 2017). This implies that central circuits are faced with an important signal detection problem: how to distinguish spikes generated by contact with external objects from spikes generated by self-motion of the sense organ. Whisking-evoked activity remains prominent in both brainstem and thalamus (Moore et al., 2015; Urbain et al., 2015; Yu et al., 2016). However, in barrel cortex, there is a marked transformation, by which the layer 4 response to

touch is robust, but that to self-motion is substantially attenuated (Hires et al., 2015). During whisking against a pole, 70% of spikes occur within 40 ms of touch onset; Hires et al., 2015). Yu et al. (2016) have identified circuitry inside layer 4 that accomplishes this transformation. The basic principle, first proposed by Simons and colleagues to account for responses to whisker deflection in anesthetized rats (Pinto et al., 2003), is that, whereas self-motion elicits relatively asynchronous firing across thalamic neurons, touch elicits a precisely timed volley of synchronous thalamic activity. The thalamic touch response is likely to reflect the strong sensitivity of thalamic neurons to $\dot{M}_0$ (Petersen et al., 2008; Bale et al., 2015b). This synchronous volley can activate layer 4 excitatory neurons before the gate is shut by feedforward inhibition (Gutnisky et al., 2017). Thalamic synchrony is important for driving cortical responses also in the visual system (Alonso et al., 1996) and may play a general role in thalamo-cortical function.

An important, general computational problem faced by the central nervous system is to extract meaningful behavioral information embedded in the population activity of PWAs. Behavioral/modeling studies have clarified the nature of the computational problem. First, whisking is active not only in the sense that whiskers move, but also in the sense that animals can control various parameters of whisking to suit a particular behavioral task (Carvell and Simons, 1995; Mitchinson et al., 2007; Hill et al., 2008; O'Connor et al., 2010a; Arkley et al., 2014; Maravall and Diamond, 2014; Sofroniew et al., 2014; Prescott et al., 2015). Thus, the forces acting on the whiskers depend not only on the structure of the external environment, but also on the current setting of the animal's whisking control parameters (amplitude, frequency and set-point). This has been illustrated by work on texture discrimination using whiskered robots (Pearson et al., 2011; Prescott et al., 2015). Here an artificial whisker is moved against a textured surface or pole to test the sufficiency of different models of sensory processing. Algorithms trained to discriminate textured surfaces fail when contact speed, or angle, is varied between trials, or if contact time is unknown (Fend et al., 2003; Evans et al., 2009; Fox et al., 2009). A potential solution to this problem is suggested by recent work that protraction against an object can be thought of as tracing out an orbit in multi-dimensional mechanical space (Bagdasarian et al., 2013). This force orbit is affected not only by the location of an object, but also by its shape, texture and compliance. Whisking against objects with different surface texture yields characteristic patterns of whisker motion (Arabzadeh et al., 2005) which can be interpreted as orbits of bending moment (Huet et al., 2015). Whisking against an object whose location varies in the horizontal plane also yields informative orbits (Bagdasarian et al., 2013). For example, although neither axial force nor bending moment uniquely encodes the radial location of object contact, the ratio of the two does (Solomon and Hartmann, 2011; Pammer et al., 2013).

Evidence is beginning to emerge for distinct functions of the cortex beyond transmission of peripheral touch information. First, coding in the extragranular layers differs markedly from that of layer 4. In infragranular layers, the touch response is much less distinct than that in layer 4, suggesting that the activity of layer 5 neurons is strongly influenced by non-sensory inputs (Hires et al., 2015). One important component of this is likely to be of motor origin (Xu et al., 2012). Second, and perhaps related, it has been observed that barrel cortex neurons of mice, trained to detect single-whisker deflections, exhibit non-sensory driven spiking, which correlates with animal choice (Yang et al., 2015). Third, recordings of cortical activity during a wall-following task (Sofroniew et al., 2014) have shown that neurons exhibit a variety of tuning functions to the distance between wall and snout: for some neurons, firing rate increases as a function of wall distance; for others it decreases and for still others the relation is complex and non-monotonic (Sofroniew et al., 2015). Since whiskers typically bend more, the closer the snout is to a wall, these findings are hard to interpret, in a simple way, on purely mechanical grounds. The task may recruit cortical circuitry, perhaps based on cross-columnar or cross laminar inhibition, which substantially transforms the peripheral drive. Finally, studies that selectively record from barrel cortex neurons that project to M1 or S2 have reported intriguing evidence for differential representation of touch signals across the two pathways that is task-dependent (Chen et al., 2013).

CONCLUSION

Experimental advances have led to a substantial advance in our understanding of somatosensation, converging on a description of 'what the whiskers tell the brain' rooted in mechanical forces. Diverse properties of primary whisker afferents, from a series of paradigms – passive stimulation, artificial whisking and awake recordings – can be accounted for by a common mechanical framework for whisker mechanoreceptor function. The fundamental driver of responses during whisker–object contact is the bending moment at the whisker base, with axial and lateral force likely to play an auxiliary role. The fundamental drivers during contact-free whisking are inertial moment and muscle contraction force.

There are a number of important directions for future work. First, the relationship between the full complement of forces/moments that characterize quasi-static whisker–object contact in 3D and neuronal activity has yet to be determined. Second, despite notable progress related to Merkel cells, the specific mechanical roles of the diverse mechanoreceptive nerve endings that innervate the whisker follicle are unclear. Third, most studies of whisker mechanics have focussed on an experimental paradigm, such as whisking against a smooth pole, that is well-described by the quasi-static approximation. However, whisking against objects with more complex shape/texture involves dynamic effects such as slip-sticks. The mechanical basis for how primary whisker afferents respond to whisking against complex objects is poorly understood. Future work, employing simultaneous measurement of neuronal

activity and of whisker–object forces has potential for substantially enriching our understanding of touch.

Acknowledgments—We thank T. Waigh and anonymous reviewers for feedback on the manuscript; E. Ahissar and D. O'Connor for discussion. This work was funded by Biotechnology and Biological Sciences Research Council (BB/L007282/1, BB/P021603/1) and Medical Research Council (MR/L01064X7/1, MR/P005659/1).

REFERENCES

Alonso J-M, Usrey WM, Reid RC (1996) Precisely correlated firing in cells of the lateral geniculate nucleus. Nature 383:815–819. Available at: http://www.sunyopt.edu/research/alonso/Precisely correlated firing in cells of the lateral genicul.pdf..

Arabzadeh E, Petersen RS, Diamond ME (2003) Encoding of whisker vibration by rat barrel cortex neurons: implications for texture discrimination. J Neurosci 23:9146–9154. Available at: http://www.ncbi.nlm.nih.gov/pubmed/14534248.

Arabzadeh E, Zorzin E, Diamond ME (2005) Neuronal encoding of texture in the whisker sensory pathway. PLoS Biol 3.

Arkley K, Grant RA, Mitchinson B, Prescott TJ (2014) Strategy change in vibrissal active sensing during rat locomotion. Curr Biol 24:1507–1512. https://doi.org/10.1016/j.cub.2014.05.036.

Armstrong-James M, Fox K (1987) Spatiotemporal convergence and divergence in the rat S1 Barrel cortex. J Comp Neurol 263:265–281.

Armstrong-James M, Fox K, Das-Gupta A (1992) Flow of excitation within rat barrel cortex on striking a single vibrissa. J Neurophysiol 68:1345–1358. Available at: http://www.ncbi.nlm.nih.gov/pubmed/1432088.

Bagdasarian K, Szwed M, Knutsen PM, Deutsch D, Derdikman D, Pietr M, Simony E, Ahissar E (2013) Pre-neuronal morphological processing of object location by individual whiskers. Nat Neurosci 16:622–631. Available at: http://dx.doi.org/10.1038/nn.3378, http://www.ncbi.nlm.nih.gov/pubmed/23563582.

Bale MR, Maravall M (2018) Organization of sensory feature selectivity in the whisker system. Neuroscience 368:70–80.

Bale MR, Petersen RS (2009) Transformation in the neural code for whisker deflection direction along the lemniscal pathway. J Neurophysiol 102:2771–2780. Available at: http://www.pubmedcentral.nih.gov/articlerender.fcgi?artid=2777830&tool=pmcentrez&rendertype=abstract.

Bale MR, Davies K, Freeman OJ, Ince RAA, Petersen RS (2013) Low-dimensional sensory feature representation by trigeminal primary afferents. J Neurosci 33:12003–12012. Available at: http://www.pubmedcentral.nih.gov/articlerender.fcgi?artid=3713733&tool=pmcentrez&rendertype=abstract.

Bale MR, Campagner D, Erskine A, Petersen RS (2015a) Microsecond-Scale Timing Precision in Rodent Trigeminal Primary Afferents. J Neurosci 35:5935–5940. Available at: http://www.jneurosci.org/cgi/doi/10.1523/JNEUROSCI.3876-14.2015.

Bale MR, Ince RAA, Santagata G, Petersen RS (2015b) Efficient population coding of naturalistic whisker motion in the ventro-posterior medial thalamus based on precise spike timing. Front Neural Circuits 9:1–14. Available at: http://journal.frontiersin.org/Article/10.3389/fncir.2015.00050/abstract.

Berg RW, Kleinfeld D (2003) Rhythmic whisking by rat: retraction as well as protraction of the vibrissae is under active muscular control. J Neurophysiol 89:104–117. Available at: http://jn.physiology.org/cgi/doi/10.1152/jn.00600.2002, http://www.ncbi.nlm.nih.gov/pubmed/12522163.

Bermejo R, Houben D, Zeigler HP (1998) Optoelectronic monitoring of individual whisker movements in rats. J Neurosci Methods 83:89–96.

Bermejo R, Vyas A, Zeigler HP (2002) Topography of rodent whisking–I. Two-dimensional monitoring of whisker movements. Somatosens Mot Res 19:341–346. Available at: http://www.ncbi.nlm.nih.gov/pubmed/12590835.

Birdwell JA, Solomon JH, Thajchayapong M, Taylor MA, Cheely M, Towal RB, Conradt J, Hartmann MJZ (2007) Biomechanical models for radial distance determination by the rat vibrissal system. J Neurophysiol 98:2439–2455.

Boubenec Y, Shulz DE, Debrégeas G (2012) Whisker encoding of mechanical events during active tactile exploration. Front Behav Neurosci 6:74. Available at: doi: 10.3389/fnbeh.2012.00074.

Bush NE, Schroeder CL, Hobbs JA, Yang AE, Huet LA, Solla SA, Hartmann MJ (2016) Decoupling kinematics and mechanics reveals coding properties of trigeminal ganglion neurons in the rat vibrissal system. eLife 5:1–23. Available at: http://elifesciences.org/lookup/doi/10.7554/eLife.13969.

Campagner D, Evans MH, Bale MR, Erskine A, Petersen RS (2016) Prediction of primary somatosensory neuron activity during active tactile exploration. Elife 5:1–18.

Carvell GE, Simons DJ (1990) Biometric analyses of vibrissal tactile discrimination in the rat. J Neurosci 10:2638–2648. Available at: Available from: http://www.jneurosci.org/cgi/content/abstract/10/8/2638.

Carvell GE, Simons DJ (1995) Task- and subject-related differences in sensorimotor behavior during active touch. Somatosens Mot Res 12:1–9. Available at: http://www.ncbi.nlm.nih.gov/pubmed/7571939 [Accessed April 24, 2017].

Chen JL, Carta S, Schneider B (2013) Behaviour-dependent recruitment of long-range projection neurons in somatosensory cortex. Nature Available at:. https://doi.org/10.1038/nature12236.

Clack NG, O'Connor DH, Huber D, Petreanu L, Hires A, Peron S, Svoboda K, Myers EW (2012) Automated tracking of whiskers in videos of head fixed rodents. PLoS Comput Biol 8.

Dandekar K, Raju BI, Srinivasan MA (2003) 3-D finite-element models of human and monkey fingertips to investigate the mechanics of tactile sense. J Biomech Eng 125:682–691.

Ebara S, Kumamoto K, Matsuura T, Mazurkiewicz JE, Rice FL (2002) Similarities and differences in the innervation of mystacial vibrissal follicle-sinus complexes in the rat and cat: A confocal microscopic study. J Comp Neurol 449:103–119. Available at: http://doi.wiley.com/10.1002/cne.10277.

Estebanez L, El Boustani S, Destexhe A, Shulz DE (2012) Correlated input reveals coexisting coding schemes in a sensory cortex. Nat Neurosci 15:1691–1699. Available at: http://www.ncbi.nlm.nih.gov/pubmed/23160042 [Accessed October 19, 2013].

Evans M, Fox CW, Pearson MJ, Prescott TJ (2009) Spectral Template Based Classification of Robotic Whisker Sensor Signals in a Floor Texture Discrimination Task. Proc Towar Auton Robot Syst:19–24.

Fend M, Bovet S, Yokoi H, Pfeifer R (2003) An active artificial whisker array for texture discrimination. Proc IEEE/RSJ Int Conf Intell Robot Syst (IROS 2003) 2:1044–1049.

Fox K (2008) Barrel Cortex. Cambridge Univ Press Available at:. https://doi.org/10.1038/nature13873.

Fox CW, Mitchinson B, Pearson MJ, Pipe AG, Prescott TJ (2009) Contact type dependency of texture classification in a whiskered mobile robot. Auton Robots 26:223–239.

Gibson JM, Welker WI (1983) Quantitative studies of stimulus coding in first-order vibrissa afferents of rats. 1. Receptive field properties and threshold distributions. Somatosens Res 1:51–67.

Grant RA, Mitchinson B, Fox CW, Prescott TJ (2009) Active touch sensing in the rat: anticipatory and regulatory control of whisker movements during surface exploration.:862–874.

Gutnisky DA, Yu J, Hires SA, To M, Bale M, Svoboda K, Golomb D (2017) Mechanisms underlying a thalamocortical transformation during active tactile sensation.

Hartmann M (2015) Vibrissa mechanical properties. Scholarpedia 10(5):6636.

Hartmann MJ, Johnson NJ, Towal RB, Assad C (2003) Mechanical characteristics of rat vibrissae: resonant frequencies and damping in isolated whiskers and in the awake behaving animal. J Neurosci 23:6510–6519.

Hill DN, Bermejo R, Zeigler HP, Kleinfeld D (2008) Biomechanics of the vibrissa motor plant in rat: rhythmic whisking consists of triphasic neuromuscular activity. J Neurosci 28:3438–3455. Available at: doi: 10.1523/JNEUROSCI.5008-07.2008.

Hires SA, Gutnisky DA, Yu J, Connor DHO, Svoboda K (2015) Low-noise encoding of active touch by layer 4 in the somatosensory cortex.:1–18

Hires SA, Schuyler A, Sy J, Huang V, Wyche I, Wang X, Golomb D (2016) Beyond cones: An improved model of whisker bending based on measured mechanics and tapering. J Neurophysiol. 90089:jn.00511.2015 Available at: http://jn.physiology.org/lookup/doi/10.1152/jn.00511.2015.

Huber D, Gutnisky DA, Peron S, O'Connor DH, Wiegert JS, Tian , Oertner TG, Looger LL, Svoboda K, L, Oertner TG, Looger LL, Svoboda K (2012) Multiple dynamic representations in the motor cortex during sensorimotor learning. Nature 484:473–478. Available at: http://www.ncbi.nlm.nih.gov/pubmed/22538608.

Huet LA, Hartmann MJZ (2016) Simulations of a Vibrissa Slipping along a Straight Edge and an Analysis of Frictional Effects during Whisking. IEEE Trans Haptics 9:158–169.

Huet LA, Schroeder CL, Hartmann MJZ (2015) Tactile signals transmitted by the vibrissa during active whisking behavior. J Neurophysiol 113:3511–3518. Available at: http://jn.physiology.org/lookup/doi/10.1152/jn.00011.2015.

Ibrahim L, Wright EA (1975) The growth of rats and mice vibrissae under normal and some abnormal conditions. J Embryol Exp Morphol 33:831–844. Available at: http://www.ncbi.nlm.nih.gov/pubmed/1176877.

Jadhav SP, Wolfe J, Feldman DE (2009) Sparse temporal coding of elementary tactile features during active whisker sensation. Nat Neurosci 12:792–800. Available at:Available from: http://www.ncbi.nlm.nih.gov/pubmed/19430473.

Jones LM, Lee S, Trageser JC, Simons DJ, Keller A (2004) Precise temporal responses in whisker trigeminal neurons. J Neurophysiol 92:665–668. Available at: http://jn.physiology.org/cgi/doi/10.1152/jn.00031.2004, http://www.pubmedcentral.nih.gov/articlerender.fcgi?artid=2800049&tool=pmcentrez&rendertype=abstract.

Khatri V, Bermejo R (2009) Whisking in air: encoding of kinematics by trigeminal ganglion neurons in awake rats. J Neurophysiol:1836–1846. Available at: http://jn.physiology.org/content/101/4/1836.short.

Knutsen PM, Ahissar E (2009) Orthogonal coding of object location. Trends Neurosci 32:101–109. Available at: http://www.ncbi.nlm.nih.gov/pubmed/19070909 [Accessed January 18, 2015].

Knutsen PM, Derdikman D, Ahissar E (2005) Tracking whisker and head movements in unrestrained behaving rodents. J Neurophysiol 93:2294–2301. Available at: doi: 10.1152/jn.00718.2004.

Knutsen PM, Biess A, Ahissar E (2008) Vibrissal Kinematics in 3D: Tight Coupling of Azimuth, Elevation, and Torsion across Different Whisking Modes. Neuron 59:35–42.

Kwegyir-Afful EE, Marella S, Simons DJ (2008) Response properties of mouse trigeminal ganglion neurons. Somatosens Mot Res 25:209–221. Available at:Available from: http://www.pubmedcentral.nih.gov/articlerender.fcgi?artid=2597100&tool=pmcentrez&rendertype=abstract.

Leiser SC, Moxon KA (2006) Relationship between physiological response type (RA and SA) and vibrissal receptive field of neurons within the rat trigeminal ganglion. J Neurophysiol 95:3129–3145. Available at:Available from: http://www.ncbi.nlm.nih.gov/pubmed/16421201.

Leiser SC, Moxon K (2007) Responses of trigeminal ganglion neurons during natural whisking behaviors in the awake rat. Neuron 53:117–133. Available at:Available from: http://www.ncbi.nlm.nih.gov/pubmed/17196535.

Lichtenstein SH, Carvell GE, Simons DJ (1990) Responses of rat trigeminal ganglion neurons to movements of vibrissae in different directions. Somat Mot Res 7:47–65.

Loft MS, Evans MH, Fox S, Petersen RS (2016) A new dimension in multiple whisker tracking: imaging and tracking whisking behaviour in 3D. Progr No 14907 2016 Neurosci Meet Planner San Diego, CA Soc Neurosci 2016 Online.

Lottem E, Azouz R (2011) A unifying framework underlying mechanotransduction in the somatosensory system. J Neurosci 31:8520–8532. Available at:Available from: http://www.ncbi.nlm.nih.gov/pubmed/21653856.

Maravall M, Diamond ME (2014) Algorithms of whisker-mediated touch perception. Curr Opin Neurobiol 25:176–186. Available at: doi: http://dx.doi.org/10.1016/j.conb.2014.01.014.

Maravall M, Petersen RS, Fairhall AL, Arabzadeh E, Diamond ME (2007) Shifts in coding properties and maintenance of information transmission during adaptation in barrel cortex. PLoS Biol 5:0323–0334.

Maravall M, Alenda A, Bale MR, Petersen RS (2013) Transformation of adaptation and gain rescaling along the whisker sensory pathway. PLoS One 8.

Marr D (1982) Vision : a computational investigation into the human representation and processing of visual information. MIT Press.

Mitchinson B, Gurney KN, Redgrave P, Melhuish C, Pipe AG, Pearson M, Gilhespy I, Prescott TJ (2004) Empirically inspired simulated electro-mechanical model of the rat mystacial follicle-sinus complex. Proc Biol Sci 271:2509–2516. Available at: Available from: http://www.pubmedcentral.nih.gov/articlerender.fcgi?artid=1691889&tool=pmcentrez&rendertype=abstract.

Mitchinson B, Martin CJ, Grant RA, Prescott TJ (2007) Feedback control in active sensing : rat exploratory whisking is modulated by environmental contact.:1035–1041.

Montemurro MA, Panzeri S, Maravall M, Alenda A, Bale MR, Brambilla M, Petersen RS (2007) Role of precise spike timing in coding of dynamic vibrissa stimuli in somatosensory thalamus. J Neurophysiol 98:1871–1882. Available at:Available from: http://www.ncbi.nlm.nih.gov/pubmed/17671103.

Moore JD, Mercer Lindsay N, Deschênes M, Kleinfeld D (2015) Vibrissa Self-Motion and Touch Are Reliably Encoded along the Same Somatosensory Pathway from Brainstem through Thalamus. PLoS Biol 13:1–28.

Nashaat MA, Oraby H, Sachdev RNS, Peña LB, Dominiak S, Larkum ME (2017) Pixying behavior: a versatile real-time and post hoc automated optical tracking method for freely moving and head fixed animals, 4:1–13

Neimark MA, Andermann ML, Hopfield JJ, Moore CI (2003) Vibrissa resonance as a transduction mechanism for tactile encoding. J Neurosci 23:6499–6509. Available at:Available from: http://www.ncbi.nlm.nih.gov/pubmed/12878691.

O'Connor DH, Clack NG, Huber D, Komiyama T, Myers EW, Svoboda K (2010a) Vibrissa-based object localization in head-fixed mice. J Neurosci 30:1947–1967. Available at:Available from: http://www.ncbi.nlm.nih.gov/pubmed/20130203.

O'Connor DH, Peron SP, Huber D, Svoboda K (2010b) Neural activity in barrel cortex underlying vibrissa-based object localization in mice. Neuron 67:1048–1061. Available at:Available from: http://www.ncbi.nlm.nih.gov/pubmed/20869600.

O'Connor DH, Hires SA, Guo ZV, Li N, Yu J, Sun Q-Q, Huber D, Svoboda K (2013) Neural coding during active somatosensation revealed using illusory touch. Nat Neurosci 16:958–965. Available at:Available from: http://www.ncbi.nlm.nih.gov/pubmed/23727820.

Pammer L, O'Connor DH, Hires SA, Clack NG, Huber D, Myers EW, Svoboda K (2013) The mechanical variables underlying object localization along the axis of the whisker. J Neurosci 33:6726–6741. Available at:Available from: http://www.pubmedcentral.nih.gov/articlerender.fcgi?artid=3733083&tool=pmcentrez&rendertype=abstract.

Panzeri S, Petersen RS, Schultz SR, Lebedev M, Diamond ME (2001) The role of spike timing in the coding of stimulus location in rat somatosensory cortex. Neuron 29:769–777. Available at: Available from: http://www.ncbi.nlm.nih.gov/pubmed/11301035.

Pearson MJ, Mitchinson B, Sullivan JC, Pipe AG, Prescott TJ (2011) Biomimetic vibrissal sensing for robots. Philos Trans R Soc London B Biol Sci 366:3085–3096.

Perkon I, Kosir A, Itskov PM, Tasic J, Diamond ME (2011) Unsupervised quantification of whisking and head movement in freely moving rodents. J Neurophysiol 105:1950–1962.

Peron SP, Freeman J, Iyer V, Guo C, Svoboda K (2015) A Cellular Resolution Map of Barrel Cortex Activity during Tactile Behavior. Neuron:1–17. Available at: http://linkinghub.elsevier.com/retrieve/pii/S0896627315002512.

Petersen RS, Diamond ME (2000) Spatial-temporal distribution of whisker-evoked activity in rat somatosensory cortex and the coding of stimulus location. J Neurosci 20:6135–6143. Available at:Available from: http://www.ncbi.nlm.nih.gov/pubmed/10934263.

Petersen RS, Panzeri S, Diamond ME (2001) Population coding of stimulus location in rat somatosensory cortex. Neuron 32:503–514. Available at:Available from: http://www.ncbi.nlm.nih.gov/pubmed/12459298.

Petersen CCH, Hahn TTG, Mehta M, Grinvald A, Sakmann B (2003) Interaction of sensory responses with spontaneous depolarization in layer 2/3 barrel cortex. Proc Natl Acad Sci U S A 100:13638–13643. Available at:Available from: http://www.pubmedcentral.nih.gov/articlerender.fcgi?artid=263866&tool=pmcentrez&rendertype=abstract.

Petersen RS, Brambilla M, Bale MR, Alenda A, Panzeri S, Montemurro MA, Maravall M (2008) Diverse and temporally precise kinetic feature selectivity in the VPm thalamic nucleus. Neuron 60:890–903. Available at: http://www.ncbi.nlm.nih.gov/pubmed/19081382 [Accessed November 3, 2013].

Petreanu L, Gutnisky DA, Huber D, Xu N, O'Connor DH, Tian L, Looger L, Svoboda K (2012) Activity in motor-sensory projections reveals distributed coding in somatosensation. Nature 489:299–303. Available at:Available from: http://www.pubmedcentral.nih.gov/articlerender.fcgi?artid=3443316&tool=pmcentrez&rendertype=abstract.

Phillips JR, Johnson KO (1982) Tactile spatial resolution. III. A continuum mechanics model of skin predicting mechanoreceptor responses to bars, edges, and gratings. J Neurophysiol 46:1204–1225.

Pinto DJ, Brumberg JC, Simons DJ (2000) Circuit dynamics and coding strategies in rodent somatosensory cortex. J Neurophysiol 83:1158–1166. Available at:Available from: http://www.ncbi.nlm.nih.gov/pubmed/10712446.

Pinto DJ, Hartings JA, Brumberg JC, Simons DJ (2003) Cortical damping: analysis of thalamocortical response transformations in rodent barrel cortex. Cereb Cortex 13:33–44. Available at: Available from: http://www.ncbi.nlm.nih.gov/pubmed/12466213.

Prescott TJ, Mitchinson B, Lepora NF, Wilson SP, Anderson SR, Porrill J, Dean P, Fox CW, Pearson MJ, Sullivan JC, Pipe AG (2015) The robot vibrissal system: understanding mammalian sensorimotor co-ordination through biomimetics. Sensorimotor Integr Whisker Syst 0 Available at: http://link.springer.com/chapter/10.1007/978-1-4939-2975-7_10.

Quist BW, Hartmann MJZ (2012) Mechanical signals at the base of a rat vibrissa: The effect of intrinsic vibrissa curvature and implications for tactile exploration. J Neurophysiol 107:2298–2312. Available at: doi: 10.1152/jn.00372.2011.

Quist BW, Faruqi RA, Hartmann MJZ (2011) Variation in Young's modulus along the length of a rat vibrissa. J Biomech 44:2775–2781. Available at: doi: 10.1016/j.jbiomech.2011.08.027.

Quist BW, Seghete V, Huet LA, Murphey TD, Hartmann MJZ (2014) Modeling forces and moments at the base of a rat vibrissa during noncontact whisking and whisking against an object. J Neurosci 34:9828–9844. Available at:Available from: http://www.pubmedcentral.nih.gov/articlerender.fcgi?artid=4107402&tool=pmcentrez&rendertype=abstract.

Rice FL, Munger BL (1986) A comparative light microscopic analysis of the sensory innervation of the mystacial pad. II. The common fur between the vibrissae. J Comp Neurol 252:186–205.

Rice FL, Kinnman E, Aldskogius H, Johansson O, Arvidsson J (1993) The innervation of the mystacial pad of the rat as revealed by PGP 9.5 immunofluorescence. J Comp Neurol 337:366–385.

Rigosa J, Lucantonio A, Noselli G, Fassihi A, Zorzin E, Manzino F, Pulecchi F, Diamond ME (2017) Dye-enhanced visualization of rat whiskers for behavioral studies. Elife 6. e25290 Available at: http://elifesciences.org/lookup/doi/10.7554/eLife.25290.

Ritt JT, Andermann ML, Moore CI (2008) Embodied information processing: vibrissa mechanics and texture features shape micromotions in actively sensing rats. Neuron 57:599–613.

Sakurai K, Akiyama M, Cai B, Scott A, Han B, Takatoh J, Sigrist M, Arber S, Wang F (2013) The organization of submodality-specific touch afferent inputs in the vibrissa column. Cell Rep 5:87–98. Available at: doi: http://dx.doi.org/10.1016/j.celrep.2013.08.051.

Severson KS, Xu D, Van de Loo M, Bai L, Ginty DD, O'Connor DH (2017) Active Touch and Self-Motion Encoding by Merkel Cell-Associated Afferents. Neuron:1–11. Available at: http://linkinghub.elsevier.com/retrieve/pii/S0896627317302891.

Shoykhet M, Doherty D, Simons DJ (2000) Coding of deflection velocity and amplitude by whisker primary afferent neurons: implications for higher level processing. Somatosens Mot Res 17:171–180. Available at:Available from: http://www.ncbi.nlm.nih.gov/pubmed/10895887.

Simons DJ (1978) Response properties of vibrissa units in rat SI somatosensory neocortex. J Neurophysiol 41:798–820.

Sofroniew NJ, Cohen JD, Lee a K, Svoboda K (2014) Natural Whisker-Guided Behavior by Head-Fixed Mice in Tactile Virtual Reality. J Neurosci 34:9537–9550. Available at:Available from: http://www.jneurosci.org/cgi/doi/10.1523/JNEUROSCI.0712-14.2014.

Sofroniew NJ, Vlasov YA, Hires SA, Freeman J, Svoboda K (2015) Neural coding in barrel cortex during whisker-guided locomotion. Elife 4:1–19.

Solomon JH, Hartmann MJZ (2011) Radial distance determination in the rat vibrissal system and the effects of Weber's law. Philos Trans R Soc B Biol Sci 366:3049–3057.

Sripati AP, Bensmaia SJ, Johnson KO (2006) A continuum mechanical model of mechanoreceptive afferent responses to indented spatial patterns, 3852–3864.

Storchi R, Bale MR, Biella GEM, Petersen RS (2012) Comparison of latency and rate coding for the direction of whisker deflection in the subcortical somatosensory pathway. J Neurophysiol 108:1810–1821. Available at:Available from: http://www.pubmedcentral.nih.gov/articlerender.fcgi?artid=3545005&tool=pmcentrez&rendertype=abstract.

Stüttgen MC, Kullmann S, Schwarz C (2008) Responses of rat trigeminal ganglion neurons to longitudinal whisker stimulation. J Neurophysiol 100:1879–1884.

Szwed M, Bagdasarian K, Ahissar E (2003) Encoding of vibrissal active touch. Neuron 40:621–630. Available at:Available from: http://www.ncbi.nlm.nih.gov/pubmed/14642284.

Szwed M, Bagdasarian K, Blumenfeld B, Barak O, Derdikman D, Ahissar E (2006) Responses of trigeminal ganglion neurons to the radial distance of contact during active vibrissal touch. J Neurophysiol 95:791–802.

Takatoh J, Prevosto V, Wang F (2017) Vibrissa sensory neurons: linking distinct morphology to specific physiology and function. Neuroscience. Available at:Available from: http://linkinghub.elsevier.com/retrieve/pii/S0306452217304384.

Tonomura S, Ebara S, Bagdasarian K, Uta D, Ahissar E, Meir I, Lampl I, Kuroda D, Furuta T, Furue H, Kunamoto K (2015) Structure-function correlations of rat trigeminal primary neurons: Emphasis on club-like endings, a vibrissal mechanoreceptor. Proc Jpn Acad, Ser B 91:560–576.

Urbain N, Salin PA, Libourel PA, Comte JC, Gentet LJ, Petersen CCH (2015) Whisking-Related Changes in Neuronal Firing and Membrane Potential Dynamics in the Somatosensory Thalamus of Awake Mice. Cell Rep 13:647–656. Available at: doi: 10.1016/j.celrep.2015.09.029.

Venkatraman S, Elkabany K, Long JD, Yao Y, Carmena JM (2009) A system for neural recording and closed-loop intracortical microstimulation in awake rodents. IEEE Trans Biomed Eng 56:15–22.

Voigts J, Sakmann B, Celikel T (2008) Unsupervised whisker tracking in unrestrained behaving animals. J Neurophysiol 100:504–515. Available at: doi: 10.1152/jn.00012.2008.

Wallach A, Bagdasarian K, Ahissar E (2016) On-going computation of whisking phase by mechanoreceptors. Nat Neurosci 19:487–493. Available at: doi: 10.1038/nn.4221.

Wallach A, Ebara S, Ahissar E (2017) What Do Sensory Organs Tell the Brain? Neuron 94:423–425. Available at: doi: 10.1016/j.neuron.2017.04.031.

Wang Q, Webber RM, Stanley GB (2010) Thalamic synchrony and the adaptive gating of information flow to cortex. Nat Neurosci 13:1534–1541. Available at: http://www.nature.com/neuro/journal/v13/n12/full/nn.2670.html, http://www.nature.com/neuro/journal/v13/n12/pdf/nn.2670.pdf..

Welker WI (1964) Analysis of sniffing of the albino rat. Behaviour 22 (3):223–244.

Whiteley SJ, Knutsen PM, Matthews DW, Kleinfeld D (2015) Deflection of a vibrissa leads to a gradient of strain across mechanoreceptors in a mystacial follicle. J Neurophysiol. n.00179.2015 Available at: doi: 10.1152/jn.00179.2015.

Williams CM, Kramer EM (2010) The advantages of a tapered whisker. PLoS One 5.

Wolfe J, Hill DN, Pahlavan S, Drew PJ, Kleinfeld D, Feldman DE (2008) Texture coding in the rat whisker system: slip-stick versus differential resonance. PLoS Biol 6. e215 Available at: http://www.pubmedcentral.nih.gov/articlerender.fcgi?artid=2525689&tool=pmcentrez&rendertype=abstract [Accessed November 11, 2013].

Wooldridge J (2012) Introductory Econometrics. A Modern Approach, 5th ed. South-western, CENGAGE Learning.

Xu N, Harnett MT, Williams SR, Huber D, Connor DHO, Svoboda K, Magee JC (2012) Nonlinear dendritic integration of sensory and motor input during an active sensing task. Nature 492:247–251. Available at: doi: 10.1038/nature11601.

Yang H, Kwon SE, Severson KS, O'Connor DH (2015) Origins of choice-related activity in mouse somatosensory cortex. Nat Neurosci 19:127–134. Available at:Available from: http://www.nature.com/neuro/journal/v19/n1/full/nn.4183.html?WT.ec_id=NEURO-201601&spMailingID=50354006&spUserID=Njk2Njk2MzE4MjUS1&spJobID=824237578&spReportId=ODI0MjM3NTc4S0.

Yu J, Gutnisky DA, Hires SA, Svoboda K (2016) Layer 4 fast-spiking interneurons filter thalamocortical signals during active somatosensation. Nat Neurosci 19:1–14. Available at: http://www.nature.com/doifinder/10.1038/nn.4412, http://www.ncbi.nlm.nih.gov/pubmed/27749825.

Zucker E, Welker WI (1969) Coding of somatic sensory input by vibrissae neurons in the rat's trigeminal ganglion. Brain Res 12:138–156. Available at: http://www.ncbi.nlm.nih.gov/pubmed/5802473, http://linkinghub.elsevier.com/retrieve/pii/0006899369900614.

(Received 8 May 2017, Accepted 1 August 2017)
(Available online 24 August 2017)